

RhoA and Rac1 GTPases play major and differential roles in stromal cell–derived factor-1–induced cell adhesion and chemotaxis in multiple myeloma

Abdel Kareem Azab,¹ Feda Azab,¹ Simona Blotta,¹ Costas M. Pitsillides,² Brian Thompson,² Judith M. Runnels,¹ Aldo M. Roccaro,¹ Hai T. Ngo,¹ Molly R. Melhem,¹ Antonio Sacco,¹ Xiaoying Jia,¹ Kenneth C. Anderson,¹ Charles P. Lin,² Barrett J. Rollins,¹ and Irene M. Ghobrial¹

¹Medical Oncology, Dana-Farber Cancer Institute and ²Wellman Center for Photomedicine, Massachusetts General Hospital, Harvard Medical School, Boston, MA

The interaction of multiple myeloma (MM) cells with the bone marrow (BM) milieu plays a crucial role in MM pathogenesis. Stromal cell–derived factor-1 (SDF1) regulates homing of MM cells to the BM. In this study, we examined the role of RhoA and Rac1 GTPases in SDF1-induced adhesion and chemotaxis of MM. We found that

both RhoA and Rac1 play key roles in SDF1-induced adhesion of MM cells to BM stromal cells, whereas RhoA was involved in chemotaxis and motility. Furthermore, both ROCK and Rac1 inhibitors reduced SDF1-induced polymerization of actin and activation of LIMK, SRC, FAK, and cofilin. Moreover, RhoA and Rac1

reduced homing of MM cells to BM niches. In conclusion, we characterized the role of RhoA and Rac1 GTPases in SDF1-induced adhesion, chemotaxis, and homing of MM cells to the BM, providing the framework for targeting RhoA and Rac1 GTPases as novel MM therapy. (Blood. 2009;114:619-629)

Introduction

Multiple myeloma (MM) is the second most prevalent hematologic malignancy; it remains incurable, and the median survival time is 3 to 5 years.^{1,2} The interaction of MM cells with extracellular matrix (ECM) proteins, bone marrow (BM) stromal cells (BMSCs), and chemokines in the BM milieu plays a crucial role in MM pathogenesis and drug resistance.³⁻⁵ These molecular events are triggered either by MM cell adhesion to BMSCs and ECM or by chemokines.⁶ We have previously shown that the chemokine stromal cell–derived factor-1 (SDF1) and its receptor, CXCR4, regulate chemotaxis and homing of MM cells to the BM.⁷ Moreover, SDF1 was shown to induce MM proliferation,⁴ up-regulate VLA-4–mediated cell adhesion to both fibronectin and vascular cell adhesion molecule (VCAM)–1,⁸ and increase chemotaxis, invasion, and actin polymerization in MM cells.⁹

RhoA, Rac1, and CDC42 are guanosine triphosphatase (GTPases) and members of the Rho-GTPases family, which is a subfamily of the Ras superfamily.¹⁰ Rho GTPases have been implicated in many basic cellular processes that influence cell proliferation, motility, chemotaxis, and adhesion.¹¹ RhoA activates ROCK1 and LIMK to regulate actin cytoskeleton in the formation of stress fibers^{12,13} and also induces adhesion¹⁴ and migration¹⁵ of cancer cells. Rac1 exerts its activity through phosphorylation and activation of PAK¹⁶ and has been implicated in a wide range of biologic activities, including the control of cell growth, cytoskeletal reorganization, cell migration, and also in adhesion of endothelial cells¹⁷ and neurons¹⁸ and neutrophils.¹⁹ In this study, we examined the role of RhoA and Rac1 GTPases in SDF1-induced adhesion and migration of MM cells and sought to elucidate the cellular mechanism of cytoskeletal changes induced by SDF.

Methods

Reagents

ROCK inhibitor Y27632, Rac1 inhibitor NSC23766, pertussis toxin (PTX), phosphoinositide-3 kinase (PI3K) inhibitor LY294002, and AKT inhibitor triciribine were purchased from Calbiochem. Recombinant SDF1, VCAM, and intercellular adhesion molecule (ICAM) were purchased from R&D. RhoA and Rac1 activation kits were purchased from Millipore, including RhoA and Rac1 antibodies. All monoclonal antibodies for Western blotting and flow cytometry, except RhoA and Rac1, were purchased from Cell Signaling Technologies.

Cells

Dexamethasone-sensitive human MM cell line MM1s was kindly provided by Dr Steven Rosen (Northwestern University, Chicago, IL). The RPMI8226 and OPM2 human MM cell lines were purchased from the ATCC.

Primary MM cells and stromal cells were obtained from BM samples from patients with MM as previously described.²⁰ Informed consent was obtained from all patients and donors in accordance with the Declaration of Helsinki. Approval of these studies was obtained by the Dana-Farber Cancer Institute Institutional Review Board.

Animals

Approval of these studies was obtained by the Dana-Farber Cancer Institute and Massachusetts General Hospital Institutional Animal Care and Use Committees. Male 7- to 9-week-old severe combined immunodeficiency (SCID) mice were obtained from Charles River Laboratories. Anesthesia was performed by intraperitoneal injections of ketamine/zyllazine, and mice were killed by carbon dioxide inhalation.

Submitted January 13, 2009; accepted May 5, 2009. Prepublished online as *Blood* First Edition paper, May 14, 2009; DOI 10.1182/blood-2009-01-199281.

The online version of this article contains a data supplement.

The publication costs of this article were defrayed in part by page charge payment. Therefore, and solely to indicate this fact, this article is hereby marked "advertisement" in accordance with 18 USC section 1734.

© 2009 by The American Society of Hematology

Expression of RhoA, Rac1, and CDC42

Cells (10^6 cells/mL) from MM1s, RPMI8226, and OPM2 MM cell lines and 3 MM patient samples were fixed and permeabilized by an incubation methanol; treated with either isotype, RhoA, Rac1, or CDC42 mouse monoclonal antibodies in phosphate-buffered saline (PBS) for 1 hour; and followed by fluorescein isothiocyanate (FITC)-labeled secondary antibody. All procedures were performed in ice-cold PBS. Samples were then analyzed with the use of flow cytometry.

Gene expression profiling of RhoA, Rac1, and CDC42

Gene expression datasets from the Mayo Clinic (GEO accession GSE6477) were obtained from the Gene Expression Omnibus for analysis and generated by the use of the Affymetrix U133A platform.²¹ The data pertaining to RhoA (probe ID 200059_s_at), Rac1 (probe ID 208641_s_at), and CDC42 (probe ID 208727_s_at) were extracted for analysis. We compared the expression in normal plasma cells from BM of 15 normal subjects and MM cells from BM of 73 newly diagnosed patients with MM.

Cell viability test

Cells (1×10^6 cells/mL) from MM1s and RPMI8226 cell lines, and CD138⁺ cells from MM patient samples, and peripheral blood mononuclear cells were cultured with increasing concentrations of Y27632, NSC23766, or a combination of both for 3 or 24 hours. Cell growth was assessed by the measurement of 3-(4,5-dimethylthiazol-2-yl)-2,5-diphenyltetrazolium bromide (Chemicon International) dye absorbance.

Adhesion assays in vitro

Fibronectin-coated plates (EMD Biosciences) and plates coated with recombinant VCAM or ICAM were used. Nontissue culture plates were coated with recombinant ICAM or VCAM (10 μ g/mL) for 24 hours at 4°C and blocked with 10 mg/mL bovine serum albumin for 1 hour at 37°C. For the stromal cell and endothelial cell adhesion assay, a confluent monolayer was generated by plating 10^4 BMSCs or human umbilical vein endothelial cells (HUVECs), respectively.

MM1s, OPM2, RPMI8226, and MM patient sample cells (2×10^5 cells/mL) were serum starved for 3 hours, labeled with calcein-AM, and treated with either Y27632 (25 μ mol/L for 3 hours), NSC23766 (25 μ mol/L for 3 hours), a combination of both, or vehicle. In adhesion to recombinant proteins and HUVEC cells, MM cells were activated with SDF1 (30 nmol/L), and nonactivated cells were used as controls. Cells were added to plates coated with fibronectin, VCAM, ICAM, stromal cells, or endothelial cells. After 2 hours at 37°C, the nonadherent cells were aspirated, wells were washed with PBS, and fluorescence intensity in the wells was measured by the use of a fluorometer (Ex/Em = 485/520 nm).

Expression of adhesion molecules on stromal-cell and MM-cell surfaces

To assess the expression of VCAM and ICAM on the cell surface of stromal cells, cells (10^5) were trypsinized for 1 minute at 37°C; washed; incubated with phycoerythrin (PE) conjugates of Isotype IgG1 control, ICAM, or VCAM monoclonal antibodies; and analyzed by flow cytometry. To assess the expression of CXCR4 on MM1s, OPM2, and RPMI8226, cells (10^6) were washed, incubated with PE conjugates of isotype IgG1 control or CXCR4 monoclonal antibodies on ice for 30 minutes, and analyzed by flow cytometry.

To determine the effect of ROCK and Rac1 inhibitors on the expression of adhesion molecules on MM cells, MM1s cells (10^6) were treated with Y27632, NSC23766, or both as described previously, followed by cell activation with SDF1 (30 nmol/L for 2 hours). Cells were incubated with PE conjugates of isotype IgG1 control, VLA4, LFA1, or CXCR4 monoclonal antibodies on ice for 30 minutes and analyzed by flow cytometry.

Chemotaxis assay

Chemotaxis was determined by the use of filters (8-micron pore size) for Transwell migration assay (Costar) according to the manufacturer's instruc-

tions. MM1s, OPM2, RPMI, and MM patient sample cells (5×10^6 cells/mL) were treated with Y27632, NSC23766, or both as described previously. Then, cells were placed in the upper migration chambers in the presence of absence of 30 nmol/L SDF1 in the lower chamber. After 3 hours of incubation, cells that migrated to the lower chambers were counted by the use of flow cytometry.

Cell motility

MM1s cells (10^6 cells/mL) were plated in a 35-mm FluoroDish (WPI). Nonadherent cells were then aspirated, and adherent cells were treated with Y27632, NSC23766, or both as described previously. Plates were then left in a prewarmed chamber of the confocal microscope for equilibration. SDF1 was added (final concentration of 30 nmol/L) 1 minute after starting of image capturing, and phase contrast images were taken every second for 10 minutes. Images were compressed to AVI files by the use of ImageJ software (National Institutes of Health [NIH]).

Actin polymerization

MM1s were treated with Y27632, NSC23766, or both as described previously and stimulated with 30 nmol/L of SDF1 for 1 minute. Cells were then fixed in 2% formaldehyde for 15 minutes at room temperature, permeabilized with 0.2% saponin, and stained with 5 μ g/mL phalloidin tagged with either Alexa-Fluor-568 or FITC. Cells stained with phalloidin-FITC were analyzed by flow cytometry, and cells stained with phalloidin-Alexa-Fluor-568 were spun onto slides, mounted, and analyzed by confocal microscopy.

Transient transfection of small interfering RNA (siRNA)

MM1s cells were transiently transfected with RhoA or Rac1 siRNA SmartPool (Dharmacon) by the use of the Cell Line Nucleofector Kit V (Amaxa Biosystems) according to the manufacturer's instructions, as in previous studies.²² Scrambled siRNA was used as a mock control. After transfection, MM1s cells were subjected to western blotting, cell proliferation adhesion to fibronectin, and chemotaxis assays.

Cytoskeletal signaling

MM1s (5×10^6 cells) were serum starved for 3 hours and then stimulated with 30 nmol/L of SDF1 for 0, 1, 2, and 5 minutes. Moreover, cells were treated with Y27632, NSC23766, or both as described in "Adhesion assays in vitro" and stimulated with 30 nmol/L of SDF1 for 1 minute.

To test the interaction of RhoA and Rac1 with the PI3K signaling pathway, MM1s (5×10^6 cells) were serum starved for 3 hours, followed by treatment with PTX (200 nmol/L for 3 hours), PI3K inhibitor LY294002 (25 μ mol/L for 20 minutes), AKT inhibitor triciribine (25 μ mol/L for 3 hours) or vehicle, and then stimulated with 30 nmol/L of SDF1 for 1 minute.

Cells were then washed with ice-cold PBS, lysed on ice, and the phosphorylation of LIMK, cofilin, FAK, Src, MLC, and AKT and expression of α -tubulin were detected by immunoblotting. Lysates also were analyzed for RhoA and Rac1 activation, as described in "RhoA and Rac1 GTPases activation."

RhoA and Rac1 GTPases activation

Cells were pelleted, rinsed with ice-cold Tris-buffered saline, and lysed with 200 μ L of magnesium lysis buffer. Lysates were then centrifuged, and protein concentrations were determined by Bradford Reagent (Sigma-Aldrich) equalized for all samples. Rohtekin or PAK1 agarose-beads (20 μ g) were added to each cell lysate (150 μ L) for the pull-down of RhoA and Rac1 GTPases, respectively. Lysates and beads were incubated for 1 hour with agitation at 4°C. Beads were then pelleted by centrifugation (10 seconds, 14 000g, 4°C), and supernatant was collected for the detection of the nonactive form of the GTPases. Beads were washed twice with lysis buffer, resuspended in 30 μ L of 2X Laemmli buffer, and proteins were detected by the use of immunoblotting as previously described.²⁰

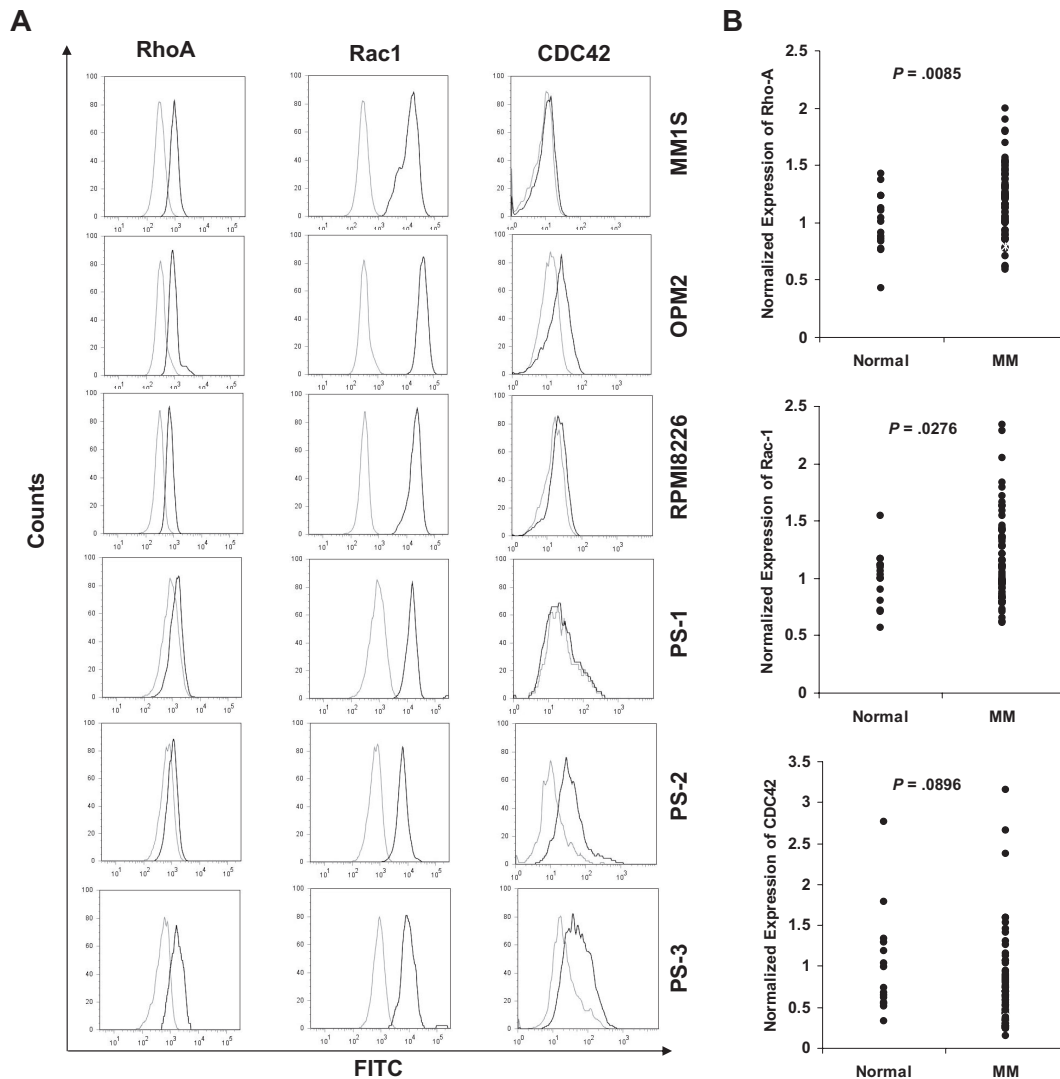


Figure 1. Gene expression of the GTPases RhoA, Rac1, and CDC42 and expression of RhoA and Rac1 in MM cell lines and patient samples. (A) Expression of RhoA and Rac1 in MM cell lines (MM1S, OPM2, and RPM18226) and 3 MM patient samples demonstrating similar expression of both GTPases in all cell lines and patient samples. (B) Gene expression of the GTPases RhoA, Rac1, and CDC42, based on NIH Gene Expression Omnibus database under the accession number GSE6691, demonstrating significant overexpression of RhoA and Rac1, but not CDC42, GTPases in MM samples compared with normal subjects.

In vivo flow cytometry

In vivo flow cytometry is a new technology that allows real-time continuous monitoring of fluorescent cells in the circulation of live animals without the need to draw blood samples. MM1s cells were treated with Y27632, NSC23766, or both as described previously and then labeled with calcein-AM. Nontreated cells were labeled with calcein-red/orange. Equal numbers (3×10^6 cells) of labeled, treated, and nontreated cells were mixed in a final volume of 150 μ L of media and injected in the tail vein of SCID mice. Mice were anesthetized, and lasers were focused on an appropriate arteriole in the mouse ear. The calcein and calcein-red/orange-labeled circulating cells were excited by 473-nm and 561-nm lasers, and signals were detected by photomultiplier tubes through 528/19-nm and 610/60-nm bandpass filters and analyzed with Matlab software. Cell counts were obtained at least every 5 minutes for 40 minutes.

In vivo confocal imaging

MM cell homing to BM vasculature of the skull was analyzed by the use of fluorescence confocal microscopy as previously described.²³ MM1s cells were treated with Y27632, NSC23766, or both as described previously; labeled with calcein; and injected to the tail vein of anesthetized SCID mice with a skin flap in their scalp to expose the underlying dorsal skull surface.

Retro-orbital injection of 20 μ L of Evans blue solution was performed immediately before imaging. Eight images of the BM niches (2 images for each niche) were captured 25 minutes after injection, and a map of the BM niches was consolidated. High-resolution images with cellular detail were obtained through the intact mouse skull by the use of a 30×0.9 NA water immersion objective lens. Calcein-labeled tumor cells and Evans blue-containing blood vessels were excited with 491-nm and 638-nm lasers and detected with photomultiplier tubes through a 528/19-nm and 680/25-nm bandpass filters, respectively. Images were taken as averaging 30 frames.

Results

Expression of RhoA, Rac1, and CDC42

We first examined the expression level of Rho, Rac, and CDC42 in MM cell lines and patient samples. Figure 1A and supplemental Table 1 (available on the *Blood* website; see the Supplemental Materials link at the top of the online article) show that both RhoA and Rac1 were expressed in all MM cell lines and patient samples; however, the expression of CDC42 was not consistent in all

samples: OPM2 and 2 patient samples showed high expression of CDC42, whereas RMP18226, MM1S, and 1 patient sample did not show CDC42 expression.

Gene expression profiling of RhoA, Rac1, and CDC42

Protein expression data obtained by flow cytometry were confirmed by the investigation of the mRNA expression of RhoA, Rac1, and CDC42 in MM by the use of gene expression profiling. The data showed a significant increase in expression of RhoA and Rac1, but not CDC42, in MM cells compared with normal plasma cells (Figure 1B).

Cell viability

Supplemental Figure 1 shows that neither the ROCK inhibitor, Rac1 inhibitor, nor their combination had any effect on cell viability of MM cell lines or patient samples after 3 hours of treatment. Moreover, at 24 hours of treatment, the ROCK inhibitor did not affect viability of cells, whereas the half maximal inhibitory concentration for the Rac1 inhibitor was 75 to 100 $\mu\text{mol/L}$. The combination of both inhibitors was similar to the effect of the Rac1 inhibitor. On the basis of those results, we used concentrations (25 $\mu\text{mol/L}$) of both inhibitors in all experiments to avoid cytotoxic effects.

Adhesion to fibronectin and BMSCs

We next examined the functional role of RhoA and Rac1 in regulating SDF1-dependent adhesion in MM. Figure 2A and B show the SDF1-induced adhesion of MM cell lines (MM1S, OPM2, and RMP18226) and patients samples, respectively, to fibronectin, which represents the ECM. Bovine serum albumin controls were used to demonstrate nonspecific adhesion. Both of the ROCK and the Rac1 inhibitors reduced MM cell adhesion to fibronectin, and their combination did not show any additive effect.

BMSCs are known to secrete SDF1, and we did not use SDF1 in these experiments. Figure 2C shows that both the ROCK and the Rac1 inhibitors reduced the adhesion of MM cell lines (MM1S, OPM2, and RMP18226) and patient samples to BMSCs.

Surface expression of adhesion molecules

We next examined the effect of SDF1 and ROCK and Rac1 inhibitors on the surface expression of CXCR4, VLA4, and LFA1 on MM1S cells. We chose VLA4 and LFA1 because they are known to be expressed on MM1S cells and regulate adhesion in MM.^{24,25} Figure 3A and supplemental Table 2 show that SDF1 induced internalization of CXCR4 receptor as expected, but that none of the inhibitors or their combination altered the effect of SDF1. In addition, neither SDF1 nor the ROCK and Rac1 inhibitors changed the surface expression of VLA4 and LFA1. We further confirmed that the integrins ICAM and VCAM were expressed on BMSCs, as shown in Figure 3B and supplemental Table 3.

The role of VLA4 and LFA1 in adhesion to BMSCs

We further show in Figure 3C that MM1S cells had minimal adhesion to immobilized recombinant ICAM, which indicates a minimal role of LFA1 in adhesion of MM1S cells. However, MM1S cells had a significantly stronger adhesion to immobilized recombinant VCAM, indicating that VLA4 plays a major role in the adhesion of MM cells. The VLA4-VCAM-mediated adhesion was increased with SDF1 and inhibited with both ROCK and Rac1 inhibitors with no additive effect of the combination. In addition, Figure 3D shows that a blocking antibody of VLA4 reduced the adhesion of MM1S cells to BMSCs. ROCK and Rac1 inhibitors did

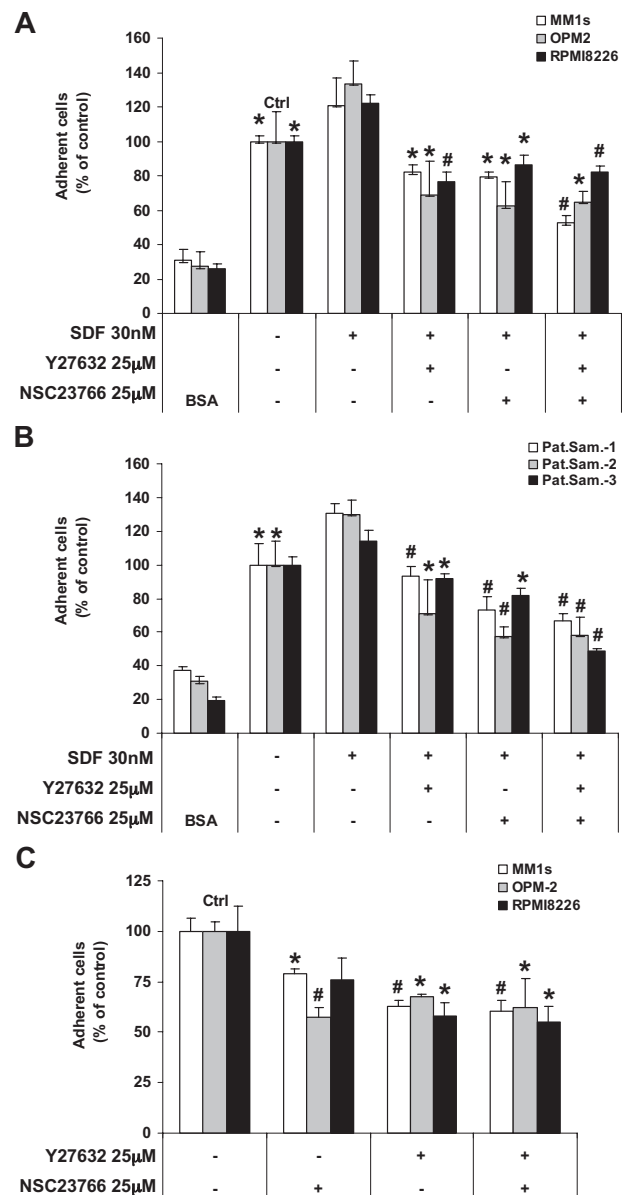


Figure 2. Effect of ROCK and Rac1 inhibitors on the SDF1-induced adhesion. Shown is the effect of ROCK and Rac1 inhibitors on the SDF1-induced adhesion of (A) MM cell lines and (B) plasma cells from MM patient samples to fibronectin and the adhesion of MM cell lines to BMSCs (C). Both the ROCK and Rac1 inhibitors decreased the adhesion of MM cells to fibronectin and BMSCs, and no additive effect was shown for their combination. Panels A and B: Groups compared with the corresponding SDF1-treated group. Panel C: Groups compared with the control, * $P < .05$; # $P < .01$.

not have additive effect with the VLA4 inhibitor, suggesting that they are affecting the same pathway.

Chemotaxis assay

Figure 4A and supplemental Table 4 show the expression of CXCR4 of the MM cell lines expressed as shift of fluorescence intensity compared with isotype control. We showed that MM cell lines demonstrated different levels of CXCR4 expression; MM1S, OPM2, and RMP18226 showed low, moderate, and high expression of CXCR4, respectively. Figure 4B and C show the chemotaxis of MM cell lines (MM1S, OPM2, and RMP18226) and patient samples, respectively. SDF1 induced chemotaxis of all MM cell lines and patient samples, and the response to SDF1 in MM cell lines was in correlation with the level of CXCR4 expression.

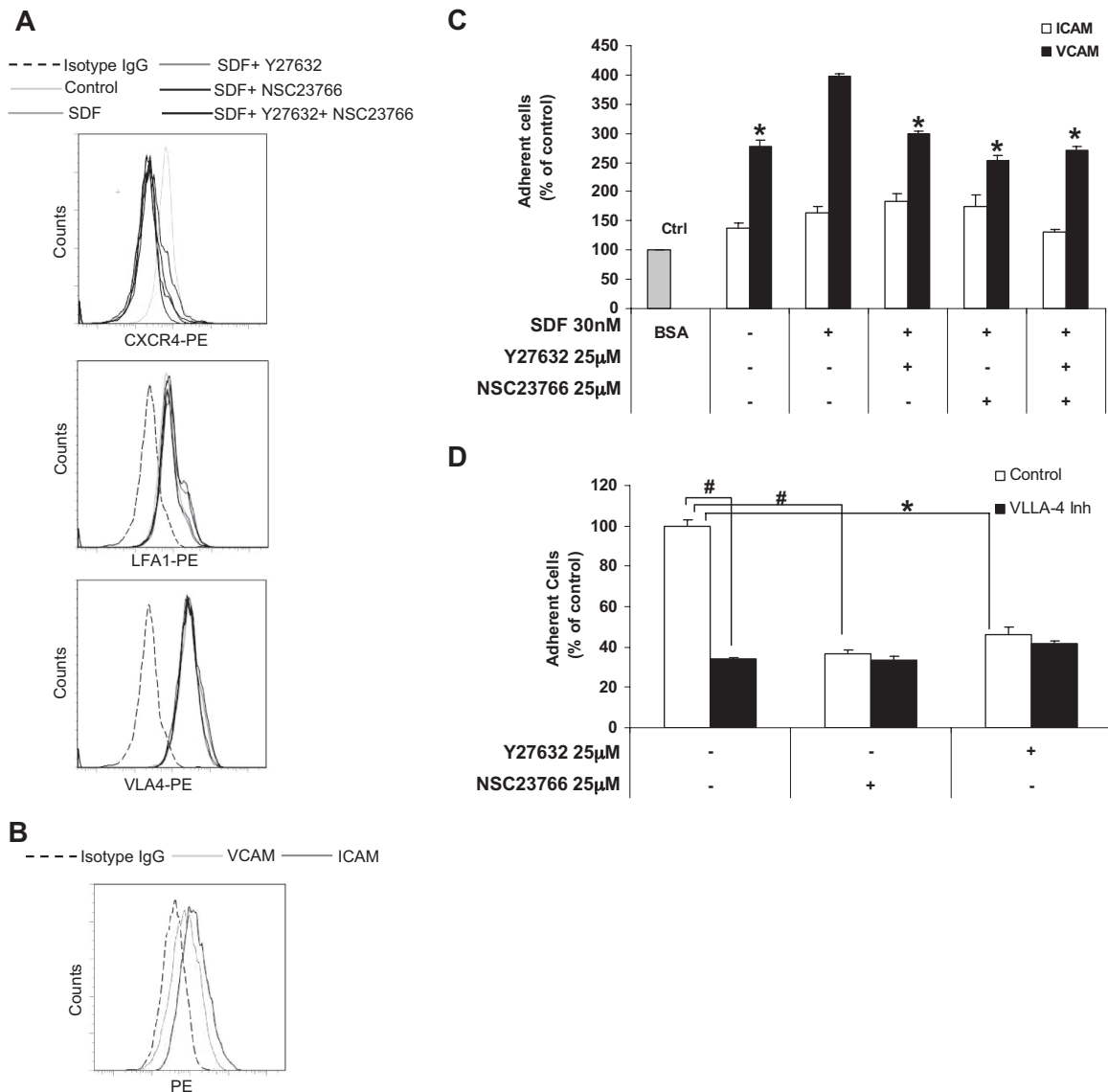


Figure 3. The effect of ROCK and Rac1 inhibitors on expression and function of adhesion molecules. (A) Effect of SDF1, ROCK, and Rac1 inhibitors on the expression of CXCR4, LFA1, and VLA4 detected by flow cytometry. It was shown that none of the inhibitors or their combination affected the internalization of CXCR4 induced by SDF1, and neither SDF1 nor any of the inhibitors affected the expression of LFA1 or VLA4 on MM1S cells. (B) The expression of ICAM and VCAM on BMSCs indicates that both molecules were expressed on BMSCs. (C) The adhesion of MM1S cells to plates coated with recombinant ICAM and VCAM shows that MM1S cells adhered to VCAM more than ICAM and that the inhibitors reduced only the adhesion of MM1S to VCAM. (D) The effect of ROCK and Rac1 inhibitors on the adhesion of MM1S cell to recombinant fibronectin in the presence or absence of VLA4 blocking antibody shows that none of the inhibitors had an additive effect beyond that of VLA4 blocking antibody. Panel C: groups compared with SDF1-treated group. * $P < .05$; # $P < .01$.

Although the treatment with Rac1 inhibitor showed minimal effect on SDF1 chemotactic effect, treatment with the ROCK inhibitor abolished this effect. The effect of the combination of the 2 inhibitors was similar to the effect of the ROCK inhibitor.

Cell motility

Supplemental Figure 2 demonstrates the effect of SDF1 (which was added after 1 minute of beginning of image capturing, 15 seconds into the supplemental videos) on the motility of MM1S cell in the presence or absence of the inhibitors. The "Control" video file shows the effect of SDF1 on nontreated MM1S cells, which were round in shape and had minimal motility before the addition of SDF1; however, the addition of SDF1 induced cell motility and a change in shape. The "NS" video shows the effect of SDF1 on cells pretreated with Rac inhibitor, showing similar results obtained in the control. The "Y" video shows the effect of SDF1 on cells

pretreated with ROCK inhibitor, showing that the inhibitor abolished the cell motility and shape changes induced by SDF1. The "Combo" video shows the effect of SDF1 on cells pretreated with combination of the inhibitors, showing similar results obtained in the ROCK inhibitor alone.

Actin polymerization

The actin polymerization was tested by detecting the interaction of phalloidin with F-actin, which was detected by confocal microscopy (Figure 4D) and flow cytometry (Figure 4E). We showed that SDF1 induced significant polarization and actin polymerization. Both the Rac1 and ROCK inhibitors reduced this effect, whereas the effect of the ROCK inhibitor was more profound. Moreover, the ROCK inhibitor, but not the Rac1 inhibitor, prevented the polarization of actin and production of filopodia. The effect of both inhibitors was similar to the effect of the ROCK inhibitor.

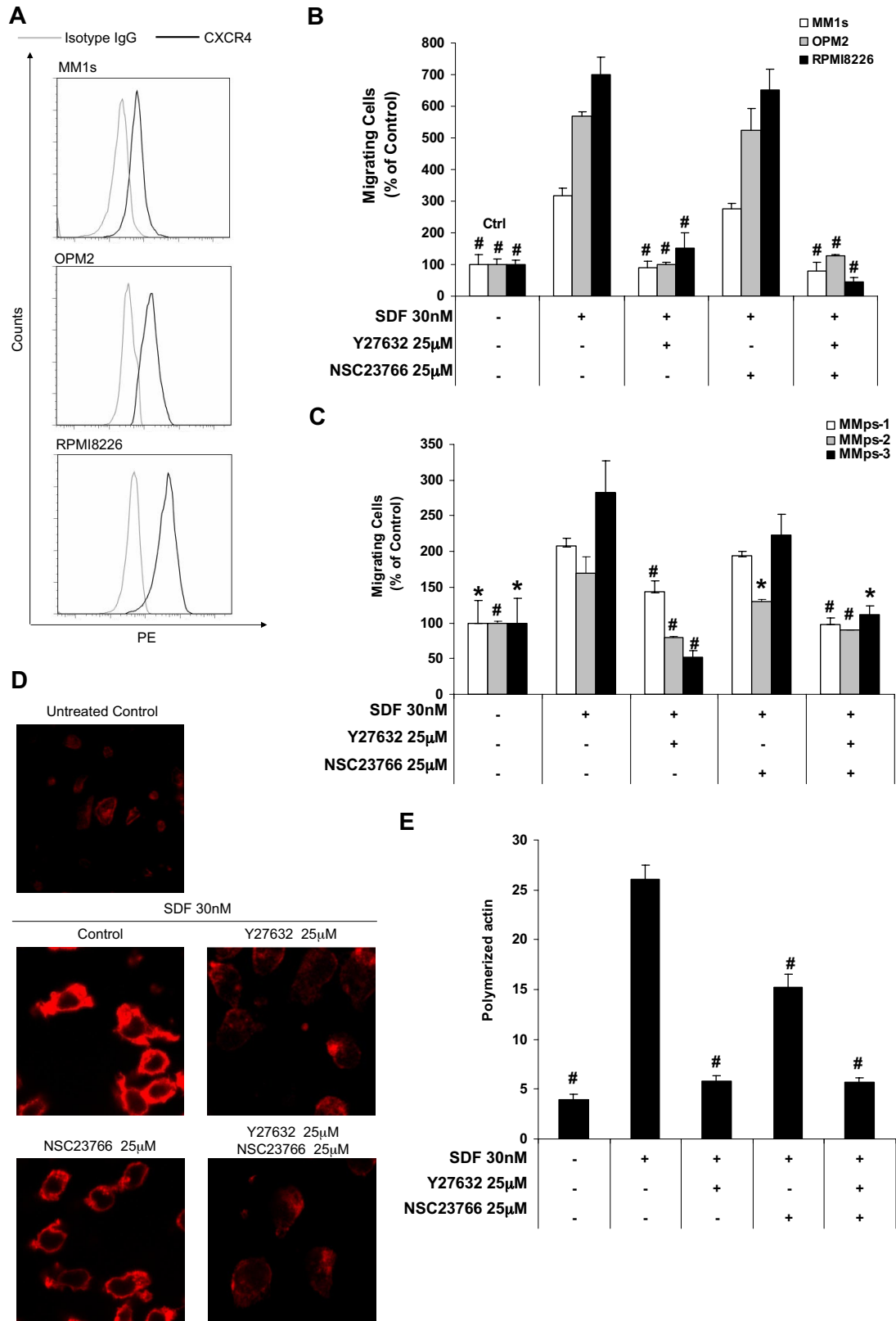
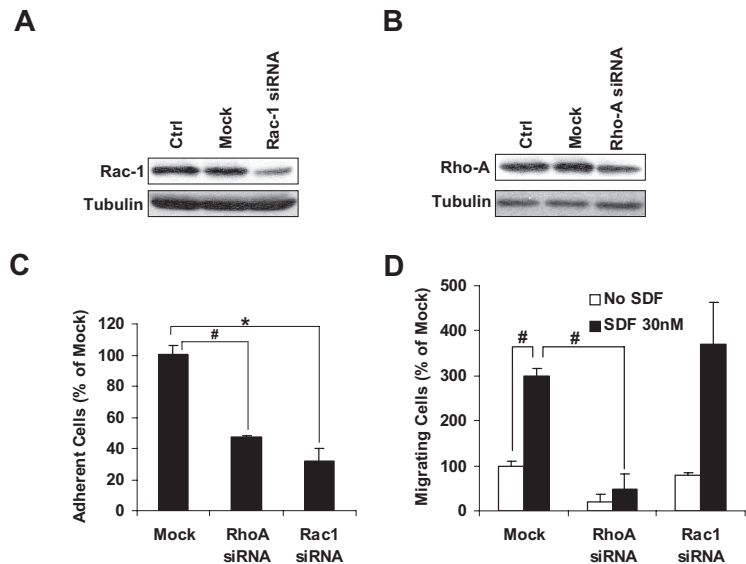


Figure 4. The effect of Rock and Rac1 inhibitors on chemotaxis and actin polymerization. (A) Expression of CXCR4 on MM cell lines (MM1S, OPM2, and RPMI8226) detected by flow cytometry showing that MM1S, OPM2, and RPMI8226 had low, intermediate, and high expression of CXCR4, respectively. (B) The effect of ROCK and Rac1 inhibitors on SDF1-induced chemotaxis of MM cell lines that was shown to correlate with the expression of CXCR4; ROCK, but not Rac1, inhibitor prevents the SDF1-induced migration of MM cells. (C) The effect of ROCK and Rac1 inhibitors on the SDF1-induced chemotaxis in MM cells from patient samples showing similar result to those obtained with the cell lines. (D) The effect of ROCK and Rac1 inhibitors on SDF1-induced actin polymerization and polarization detected by confocal microscopy and (E) flow cytometry. It was shown that both inhibitors reduced actin polymerization, but the ROCK inhibitor showed a more profound effect, and only the ROCK inhibitor prevented actin polarization. Panels A-C: Groups compared with SDF1-treated group. * $P < .05$; # $P < .01$.

Figure 5. The effect of down-regulation of RhoA and Rac1 on MM1s adhesion and chemotaxis. The effect of transient transfection of MM1s cells with siRNA on the expression of Rac1 (A) and RhoA (B) detected by immunoblotting and adhesion to fibronectin (C) and chemotaxis induced by SDF1. * $P < .05$; # $P < .01$.



Transient transfection of siRNA

To further confirm the pharmacologic effects of drug, we transiently knocked-down both Rac1 and RhoA as shown in Figure 5A and B, respectively, and we tested the effect of the knockdown on the adhesion and chemotaxis of MM1s cells. Figure 5C shows that knockdown of either RhoA or Rac1 reduced the adhesion of MM1s cells to fibronectin-coated plates. Figure 5D shows that only the knockdown of RhoA, but not Rac1, prevented the chemotactic effect of SDF1 in MM1s cells.

Cytoskeletal signaling

We found that SDF1 induced activation of RhoA and Rac1, as demonstrated by their binding to GTP, and induced phosphorylation of LIMK, cofilin, FAK, Src, MLC, and AKT. Figure 6A showed that maximal activation was obtained at 1 minute after treatment with SDF1.

Figure 6B shows that the ROCK inhibitor increased GTP activation of RhoA, whereas the Rac1 inhibitor did not alter the activation of RhoA. The combination of inhibitors showed results similar to ROCK inhibition. Both ROCK and Rac1 inhibitors reduced GTP activation of Rac1, and their combination showed an additive effect. Both inhibitors showed similar inhibition of the phosphorylation of LIMK, cofilin, FAK, and Src, and their combination did not induce additive inhibition. The phosphorylation of MLC was reduced by the ROCK inhibitor but not by the Rac1 inhibitor, and the combination of the inhibitors showed similar results to those of ROCK inhibitor alone. The phosphorylation of AKT was increased by the ROCK inhibitor and not altered by the Rac1 inhibitor, and the combination of the inhibitors showed results similar to those of the ROCK inhibitor alone.

To test the interaction of RhoA and Rac1 with the PI3K kinase signaling pathway, we studied the effect of inhibitors of AKT (triciribin), PI3K (LY294002), and Gi-protein (PTX) on the activation of RhoA and Rac1. Figure 6C shows that activation of RhoA was reduced only by PTX but not by triciribin or LY294002. The activation of Rac1 was decreased by all 3 inhibitors, indicating that Rac1 was downstream of all of them. To confirm the activity of the inhibitors, we showed that PTX reduced the phosphorylation of AKT and that triciribin and LY294002 abolished it. Moreover, both PTX and LY294002 but not triciribin reduced SDF1-induced chemotaxis of MM1s cells, as shown in Figure 6D. We then tested the effect of the ROCK and Rac1 inhibitors on chemotaxis (Figure 5E) and adhesion (Figure 6F) of MM1s cells in the presence or absence of the PI3K inhibitor LY294002. Figure 6E shows

that the Rac1 inhibitor did not alter the inhibitory effect of LY294002 on MM1s chemotaxis; however, the ROCK inhibitor had an additive effect when combined with LY294002. Figure 6F shows that the inhibitory effect of LY294002 on MM1s cell adhesion was not altered by combination with the Rac1 inhibitor and slightly decreased by the ROCK inhibitor.

Homing in vivo

To further investigate the role of RhoA and Rac1 in homing in vivo, we first tested the effect of the ROCK and Rac1 inhibitors on the adhesion of MM1s cell to human endothelial cells in vitro. Figure 7A shows that both inhibitors reduced the adhesion of MM1s cells to HUVEC cells in the presence of SDF1, and their combination showed similar results to each of the inhibitors alone. Figure 7B shows the effect of the inhibitors on the number of circulating MM1s cells after tail vein injection by the use of in vivo flow cytometry. It shows that almost all nontreated control cells exited from the circulation 25 minutes after the injection, whereas pretreatment of the cells with either or both of the inhibitors prolonged the time of circulation of MM1s cells, and approximately 50% of the cells were still circulating 30 minutes after injection. We further tested the effect of the inhibitors on homing of MM1s cells to the BM niches of the mouse skull using in vivo confocal microscopy. Supplemental Figure 3 shows a schema of the mouse skull and the structure of BM niches. Figure 7C shows that 25 minutes after the injection of nontreated MM1s cells, a high number of MM1s cells were found in the BM niches, whereas at the same time interval, there was a significantly lower number of MM1s cells pretreated with the ROCK or Rac1 inhibitors; however, the effect of the ROCK inhibitor was more profound. The combination of the inhibitors showed similar results to that obtained with the ROCK inhibitor. The cells in each image were counted, and the average number of cells per image obtained. Figure 7D depicts the difference in the number of cells counted in the BM niches after treatment with the inhibitors.

Discussion

The adhesion of MM cells to ECM proteins and BMSCs plays a crucial role in MM pathogenesis and drug resistance.^{4,5} Studies^{26,27}

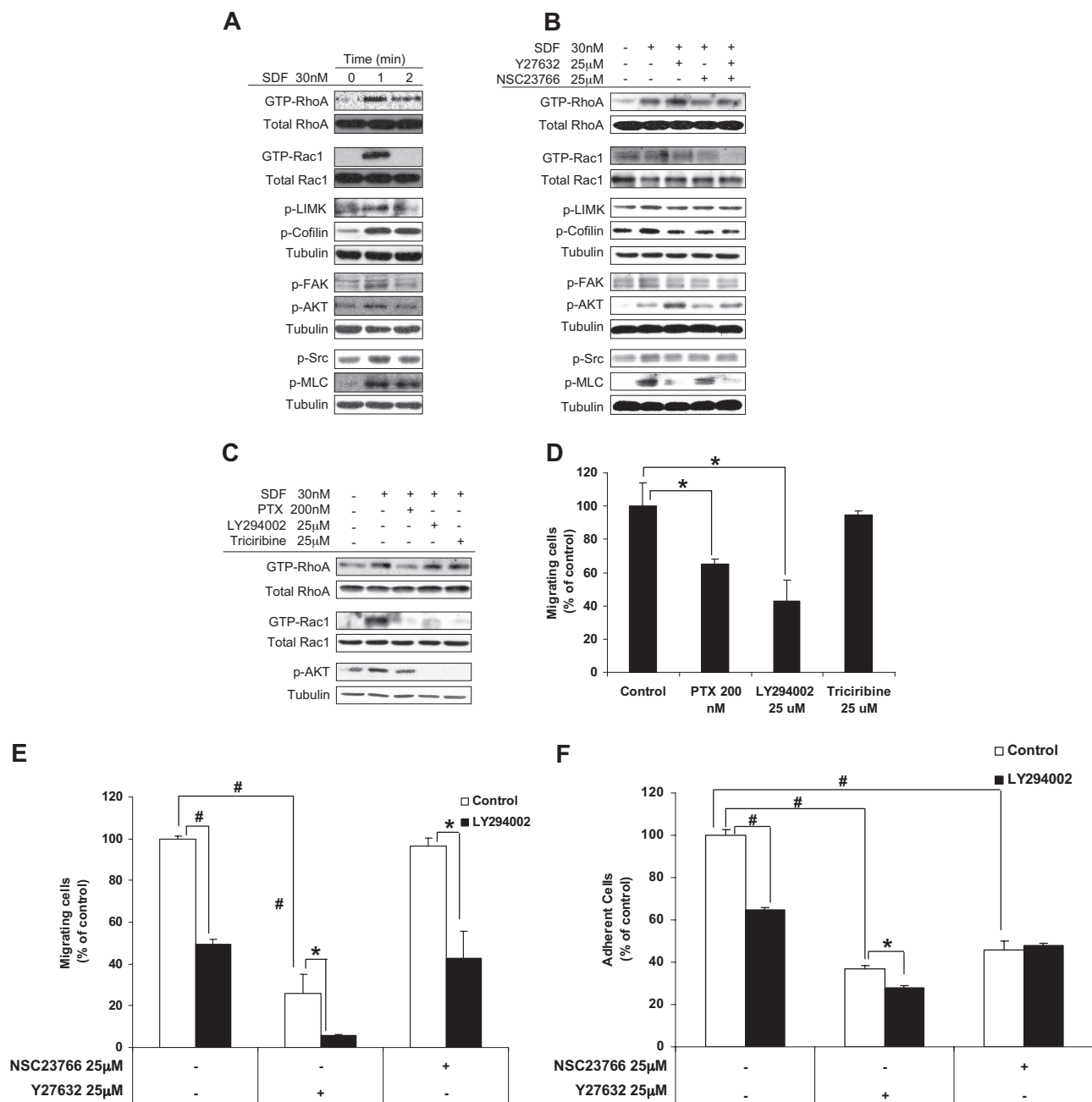


Figure 6. Characterization of the role of RhoA and Rac1 in cytoskeletal signaling. (A) The effect of SDF1 on the activation of key proteins in cytoskeletal signaling including RhoA, Rac1, LIMK, FAK, SRC, cofilin, MLC and AKT detected by immunoblotting. SDF1 was shown to induce fast activation of those proteins 1 minute after treatment. (B) The effect of ROCK and Rac1 inhibitors on the activation of cytoskeletal proteins, detected by immunoblotting. (C) The effect of inhibitors of coupling of G-protein, PI3K, and AKT on the SDF1-induced activation of RhoA and Rac1 GTPases, detected by immunoblotting. (D) The effect of inhibitors of coupling of G-protein, PI3K, and AKT on the SDF1-induced chemotaxis of MM1S cells. The effect of ROCK and Rac1 inhibitors on MM cell (E) chemotaxis and (F) adhesion to fibronectin induced by SDF1 in the presence or absence of PI3K inhibitor. **P* < .05; #*P* < .01.

have demonstrated the presence of circulating malignant plasma cells in more than 70% of patients diagnosed with MM. Homing of cells from the blood to the BM niches requires active navigation, and one of the most extensively studied chemokines for homing of MM cells is SDF1 and its receptor, CXCR4.^{28,29} To date, the mechanism in which SDF1 and CXCR4 induce adhesion and chemotaxis of MM cells to the BM is not fully understood.

Rho GTPases are key regulators of cytoskeletal dynamics and affect many cellular processes, including cell adhesion and chemotaxis. These proteins function by interacting with and stimulating various downstream targets, including actin, protein kinases, and phospholipases.³⁰ Rho GTPases have oncogenic activity and

promote cancer-cell invasion and metastasis.^{31,32} CXCR4 was shown to induce cell migration of T cells via signaling through Rho GTPases, which were therefore suggested as a potential pharmacologic target for treatment of human diseases that involve function of CXCR4.³²

In this study, we have tested the role of Rho-GTPases in SDF1-induced MM cell adhesion, chemotaxis, and homing to the BM. We first analyzed protein expression of RhoA, Rac1, and CDC42 in MM cell lines and patient samples using flow cytometry. We found that RhoA and Rac1 were highly expressed in all MM cell lines and patient samples, whereas the expression of CDC2 did not show a uniform level of expression. We further confirmed that

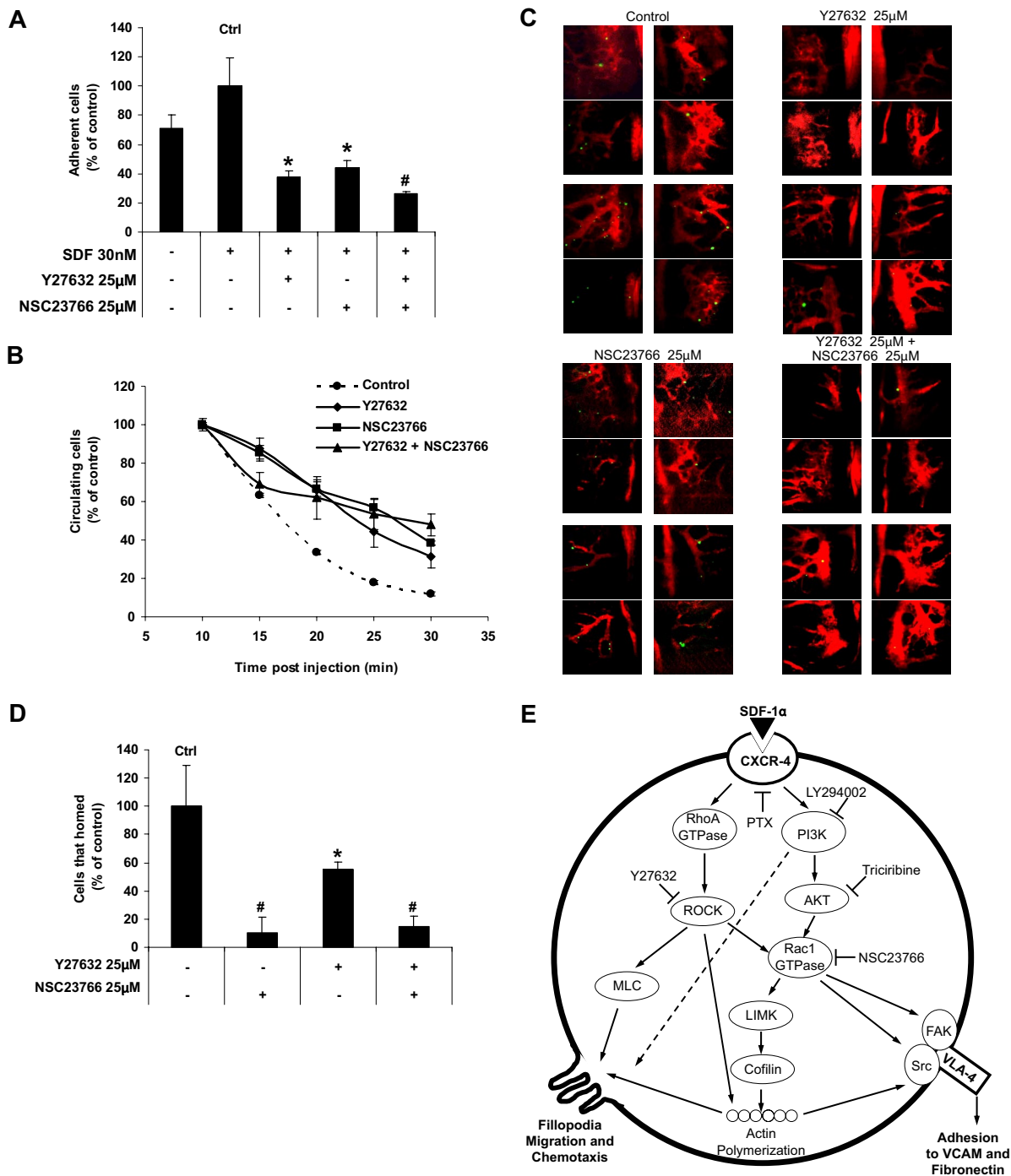


Figure 7. The effect of ROCK and Rac1 inhibitors on adhesion to endothelial cells in vitro and extravasation and homing in vivo. (A) The effect of ROCK and Rac1 inhibitors on SDF1-induced MM1S cell adhesion to plates coated with HUVEC cells in vitro showing that both inhibitors reduced the adhesion with no additive effect for the combination. (B) The effect of ROCK and Rac1 inhibitors on MM1S cell homing after tail vein injection in mice detected by detection of circulating MM1S cells with time showing that both inhibitors reduced the adhesion with no additive effect for the combination. (C) The effect of ROCK and Rac1 inhibitors on MM1S cell homing to the BM niches in mouse skull after tail vein injection demonstrating that both inhibitors prevented homing of MM1S cell to BM, whereas ROCK inhibitor had a more profound effect. (D) Quantification of the number of MM1S cell homed to BM in panel C. (E) The suggested mechanism for SDF1-induced MM cell adhesion and chemotaxis involving RhoA and Rac1. Panel A: Groups compared with the SDF1-treated group. Panel D: Groups compared with the control, **P* < .05; #*P* < .01.

the mRNA expression of RhoA and Rac1, but not CDC42, GTPases was greater in MM compared with normal plasma cells. Therefore, we focused on the role of RhoA and Rac1 GTPases in the adhesion and chemotaxis of MM cells. Specifically, we used 2 small molecule-specific inhibitors for Rac1 GTPase and for ROCK (the main effector protein downstream of RhoA) to block the signaling of Rac1 and RhoA.^{33,34} We confirmed that none of these inhibitors induce cell toxicity at the time used for functional assays (after

3 hours of treatment). Moreover, we used a concentration of both inhibitors that did not induce cell death at 24 hours of treatment.

To study the role of RhoA and Rac1 in the SDF1-induced adhesion of MM cell to the BM microenvironment, we tested the effect of the inhibitors on the adhesion of MM cell lines and patient samples to fibronectin, representing the ECM proteins. Both of the RhoA and Rac1 GTPases play key roles in adhesion to ECM. Moreover, we demonstrated a similar role in the adhesion of MM

cells to BMSCs, indicating similar targets of adhesion molecules in the ECM and BMSCs. We characterized the expression of the integrins VLA4 and LFA1, which were both expressed on MM cells, and found that the inhibition of RhoA or Rac1 pathways did not affect the expression of these integrins. Furthermore, we tested the expression of the substrates of these integrins on BMSCs and found that both VCAM and ICAM were expressed on the BMSCs. However, we found that the adhesion of MM cells to recombinant VCAM was significantly greater than their adhesion to recombinant ICAM and that the inhibitors of GTPases affected only adhesion to VCAM but not ICAM. These data indicated that SDF1-induced adhesion was mediated through RhoA and Rac1, which activated VLA4 and not FLA1. These results were confirmed by showing that the inhibitors did not enhance the effect of VLA4 blocking antibody on adhesion of MM cells. These results are in accord with previous reports indicating that SDF1 induced MM cell adhesion through VLA4.⁸ The combination of the inhibitors did not induce additional activity in reducing adhesion of MM cells to fibronectin, BMSCs, and VCAM, suggesting that both GTPases are in the same signaling pathway.

To test the role of RhoA and Rac1 GTPases in SDF1-induced chemotaxis of MM cells, we used a Transwell migration assay for MM cell lines and patient samples. We found that chemotaxis of MM cells correlated with expression of CXCR4 on those cells and that inhibition of the RhoA pathway with the ROCK inhibitor abolished the chemotactic effect of SDF1, whereas inhibiting the Rac1 pathway minimally affected the chemotaxis of MM cells. Furthermore, we confirmed this effect by testing the effect of the inhibitor on MM cell motility induced by SDF1 using confocal microscopy: inhibiting the RhoA pathway, but not the Rac1 pathway, inhibited MM cell motility induced by SDF1. The combination of the 2 inhibitors showed an effect similar to that of the ROCK inhibitor alone, indicating that RhoA, but not Rac1, GTPase plays a role in MM chemotaxis. The pharmacologic effect of the Rac1 and ROCK inhibitors were confirmed by transient down-regulation of Rac1 and RhoA pathways by knocking down Rac1 and RhoA, which both showed inhibition of adhesion, but only knocking down RhoA inhibited chemotaxis.

To investigate the molecular mechanism of the effects mentioned previously, we tested the role of SDF1, RhoA, and Rac1 on activation of key proteins in cytoskeletal signaling. We found that SDF1 induced actin polymerization and polarization in MM cells, quantified by flow cytometry and depicted by confocal microscopy. Both inhibitors reduced the polymerization of actin; however, the ROCK inhibitor had a more significant effect and abolished actin polarization. Moreover, SDF1 induced rapid phosphorylation of RhoA, Rac1, AKT, LIMK, FAK, SRC, cofilin, and MLC. The ROCK inhibitor increased the amount of GTP-activated RhoA by the blocking of downstream effector proteins. In addition, the ROCK inhibitor reduced activation of Rac1, indicating that ROCK is upstream of Rac1. The Rac1 inhibitor decreased the activation of Rac1, as expected, and did not affect the activation of RhoA and reduced the phosphorylation of LIMK, FAK, SRC, and cofilin. Moreover, both Rac1 and ROCK inhibitors reduced the activation of LIMK, SRC, FAK, and cofilin, with no further effect of the combination. These proteins are known to be involved in activating integrins and promoting adhesion, which is consistent with the similar role of RhoA and Rac1 in MM cell adhesion. Moreover, we found that ROCK but not Rac1 inhibitor reduced the activation of MLC, which is known to induce contraction of actin-myosin fibers, indicating that differential role RhoA in MM cell motility and chemotaxis. The activation of AKT was increased by the inhibition

of the ROCK inhibitor but was not altered by the Rac1 inhibitor; this observation led us to study the interaction between the PI3K pathway and the RhoA and Rac1 pathways. We assessed the effect of inhibitors of the coupling of the G proteins, PI3K, and AKT on activation of RhoA and Rac1. Inhibition of the coupling of G-protein receptor (CXCR4) by PTX reduced the activation of both RhoA and Rac1, demonstrating that they are both downstream of CXCR4.

Although both the PI3K and AKT inhibitors (LY294002 and triciribin) inhibited the activation of Rac1, they did not alter the activation of RhoA. This effect of the inhibitors on the PI3K pathway was confirmed by their inhibition of AKT activation, indicating that PI3K and RhoA are in different pathways downstream of CXCR4. Functionally, both the G-protein coupling inhibitor and PI3K inhibitor, but not the AKT inhibitor, reduced SDF1-induced chemotaxis of MM cells. Although the combination of PI3K and Rac1 inhibitors did not show an additive effect in preventing chemotaxis, an additive effect of PI3K and ROCK inhibitor was shown. These data suggest that the role of PI3K in chemotaxis is not through affecting Rac1, which is not involved in chemotaxis, or RhoA, but has an additive effect with RhoA. The PI3K inhibitor also reduced the adhesion of MM cells, but the PI3K inhibitor combination with either the ROCK or Rac1 inhibitors did not have an additive effect, suggesting that both the RhoA and the PI3K pathways promote their effect on adhesion of MM cells through Rac1 GTPase.

Finally, we tested the effect of the ROCK and Rac1 inhibitors on homing of MM cells *in vivo* to the BM of SCID mice. First, we tested the effect of the inhibitors on adhesion of MM cells to endothelial cell *in vitro* as a model for extravasation of cells *in vitro* and found that the both inhibitors reduced adhesion of MM cell to endothelial cells *in vitro* with no additive effect of the combination. Similar results were obtained *in vivo* when we tested the effect of the inhibitors on the time needed for MM cells to home to the BM by detecting the number of circulating MM cells after tail vein injection in mice using *in vivo* flow cytometry. Most of the untreated cells were not detected in the circulation 25 minutes after cell injection, whereas treatment with either of the inhibitors alone or the combination delayed the exit of cell from the circulation such that 60% of the cells were still in the circulation at 25 minutes after injection. Furthermore, *in vivo* confocal microscopy imaging of the BM niches in the skull of the mice showed that both inhibitors reduced the number of MM cells present in the BM niches; however, the effect of the ROCK inhibitor was more significant, perhaps attributable to the differential role of RhoA on MM cell chemotaxis, in addition to its role on adhesion.

In conclusion, we studied the role of RhoA and Rac1 GTPases in adhesion and chemotaxis of MM cells to the BM induced by SDF1. We found that RhoA was important for both adhesion and chemotaxis, whereas Rac1 was important for adhesion but not chemotaxis. Moreover, we have characterized the molecular mechanisms in which SDF1 induces these different functions. On the basis of these results, we suggest Rho-GTPases as potential novel therapeutic targets in MM.

Acknowledgments

This study is supported in part by R01CA125690, NIH EB000664 (Bethesda, MD), and the Leukemia & Lymphoma Society (White Plains, NY) to I.M.G.

Authorship

Contribution: A.K.A. designed and performed research, analyzed data, and wrote the paper; F.A., S.B., C.M.P., and B.T. performed research; J.M.R., A.M.R., H.T.N., M.R.M., A.S., X.J., K.C.A., C.P.L., and B.J.R. analyzed data; and I.M.G. analyzed data and wrote the paper.

Conflict-of-interest disclosure: I.M.G. and K.C.A. are on speakers bureaus for Millennium, Celgene, and Novartis. K.C.A. is an advisor for Celgene and Millennium. B.J.R. is an advisor for ProtAffin Biotechnologie AG. The remaining authors declare no competing financial interests.

Correspondence: Irene M. Ghobrial, MD, Medical Oncology, Dana-Farber Cancer Institute, 44 Binney St, Mayer 548A, Boston, MA 0211; e-mail: Irene_ghobrial@dfci.harvard.edu.

References

- Kyle RA, Rajkumar SV. Multiple myeloma. *N Engl J Med*. 2004;351:1860-1873.
- Jemal A, Tiwari RC, Murray T, et al. Cancer statistics, 2004. *CA Cancer J Clin*. 2004;54:8-29.
- Damiano JS, Cress AE, Hazlehurst LA, Shtil AA, Dalton WS. Cell adhesion mediated drug resistance (CAM-DR): role of integrins and resistance to apoptosis in human myeloma cell lines. *Blood*. 1999;93:1658-1667.
- Hideshima T, Chauhan D, Hayashi T, et al. The biological sequelae of stromal cell-derived factor-1alpha in multiple myeloma. *Mol Cancer Ther*. 2002;1:539-544.
- Hideshima T, Podar K, Chauhan D, Anderson KC. Cytokines and signal transduction. *Best Pract Res Clin Haematol*. 2005;18:509-524.
- Pagnucco G, Cardinale G, Gervasi F. Targeting multiple myeloma cells and their bone marrow microenvironment. *Ann N Y Acad Sci*. 2004;1028:390-399.
- Alsayed Y, Ngo H, Runnels J, et al. Mechanisms of regulation of CXCR4/SDF-1 (CXCL12)-dependent migration and homing in multiple myeloma. *Blood*. 2007;109:2708-2717.
- Sanz-Rodríguez F, Hidalgo A, Teixido J. Chemokine stromal cell-derived factor-1alpha modulates VLA-4 integrin-mediated multiple myeloma cell adhesion to CS-1/fibronectin and VCAM-1. *Blood*. 2001;97:346-351.
- Parmo-Cabañas M, Bartolome RA, Wright N, Hidalgo A, Dräger AM, Teixido J. Integrin alpha4beta1 involvement in stromal cell-derived factor-1alpha-promoted myeloma cell transendothelial migration and adhesion: role of cAMP and the actin cytoskeleton in adhesion. *Exp Cell Res*. 2004;294:571-580.
- Boureux A, Vignal E, Faure S, Fort P. Evolution of the Rho family of ras-like GTPases in eukaryotes. *Mol Biol Evol*. 2007;24:203-216.
- Etienne-Manneville S, Hall A. Rho GTPases in cell biology. *Nature*. 2002;420:629-635.
- Maekawa M, Ishizaki T, Boku S, et al. Signaling from Rho to the actin cytoskeleton through protein kinases ROCK and LIM-kinase. *Science*. 1999;285:895-898.
- Yiu G, He Z. Glial inhibition of CNS axon regeneration. *Nat Rev Neurosci*. 2006;7:617-627.
- Feijóo-Cuaresma M, Mendez F, Maqueda A, et al. Inadequate activation of the GTPase RhoA contributes to the lack of fibronectin matrix assembly in von Hippel-Lindau protein-defective renal cancer cells. *J Biol Chem*. 2008;283:24982-24990.
- Caramel J, Quignon F, Delattre O. RhoA-dependent regulation of cell migration by the tumor suppressor hSNF5/INI1. *Cancer Res*. 2008;68:6154-6161.
- Knaus UG, Wang Y, Reilly AM, Warnock D, Jackson JH. Structural requirements for PAK activation by Rac GTPases. *J Biol Chem*. 1998;273:21512-21518.
- Lee SH, Kunz J, Lin SH, Yu-Lee LY. 16-kDa prolactin inhibits endothelial cell migration by down-regulating the Ras-Tiam1-Rac1-Pak1 signaling pathway. *Cancer Res*. 2007;67:11045-11053.
- Chen L, Liao G, Waclaw RR, et al. Rac1 controls the formation of midline commissures and the competency of tangential migration in ventral telencephalic neurons. *J Neurosci*. 2007;27:3884-3893.
- Filippi MD, Szczur K, Harris CE, Berclaz PY. Rho GTPase Rac1 is critical for neutrophil migration into the lung. *Blood*. 2007;109:1257-1264.
- Leleu X, Jia X, Runnels J, et al. The Akt pathway regulates survival and homing in Waldenstrom macroglobulinemia. *Blood*. 2007;110:4417-4426.
- Chng WJ, Kumar S, VanWier S, et al. Molecular dissection of hyperdiploid multiple myeloma by gene expression profiling. *Cancer Res*. 2007;67:2982-2989.
- Hideshima T, Bradner JE, Wong J, et al. Small-molecule inhibition of proteasome and aggregate function induces synergistic antitumor activity in multiple myeloma. *Proc Natl Acad Sci U S A*. 2005;102:8567-8572.
- Sipkins DA, Wei X, Wu JW, et al. In vivo imaging of specialized bone marrow endothelial microdomains for tumour engraftment. *Nature*. 2005;435:969-973.
- Sanz-Rodríguez F, Teixido J. VLA-4-dependent myeloma cell adhesion. *Leuk Lymphoma*. 2001;41:239-245.
- Vacca A, Di Loreto M, Ribatti D, et al. Bone marrow of patients with active multiple myeloma: angiogenesis and plasma cell adhesion molecules LFA-1, VLA-4, LAM-1, and CD44. *Am J Hematol*. 1995;50:9-14.
- Billadeau D, Van Ness B, Kimlinger T, et al. Clonal circulating cells are common in plasma cell proliferative disorders: a comparison of monoclonal gammopathy of undetermined significance, smoldering multiple myeloma, and active myeloma. *Blood*. 1996;88:289-296.
- Nowakowski GS, Witzig TE, Dingli D, et al. Circulating plasma cells detected by flow cytometry as a predictor of survival in 302 patients with newly diagnosed multiple myeloma. *Blood*. 2005;106:2276-2279.
- Kucia M, Jankowski K, Reza R, et al. CXCR4-SDF-1 signalling, locomotion, chemotaxis and adhesion. *J Mol Histol*. 2004;35:233-245.
- Libura J, Drukala J, Majka M, et al. CXCR4-SDF-1 signaling is active in rhabdomyosarcoma cells and regulates locomotion, chemotaxis, and adhesion. *Blood*. 2002;100:2597-2606.
- Heasman SJ, Ridley AJ. Mammalian Rho GTPases: new insights into their functions from in vivo studies. *Nat Rev Mol Cell Biol*. 2008;9:690-701.
- Vega FM, Ridley AJ. Rho GTPases in cancer cell biology. *FEBS Lett*. 2008;582:2093-2101.
- Tan W, Martin D, Gutkind JS. The Galpha13-Rho signaling axis is required for SDF-1-induced migration through CXCR4. *J Biol Chem*. 2006;281:39542-39549.
- Gao Y, Dickerson JB, Guo F, Zheng J, Zheng Y. Rational design and characterization of a Rac GTPase-specific small molecule inhibitor. *Proc Natl Acad Sci U S A*. 2004;101:7618-7623.
- Uehata M, Ishizaki T, Satoh H, et al. Calcium sensitization of smooth muscle mediated by a Rho-associated protein kinase in hypertension. *Nature*. 1997;389:990-994.



blood[®]

2009 114: 619-629

doi:10.1182/blood-2009-01-199281 originally published
online May 14, 2009

RhoA and Rac1 GTPases play major and differential roles in stromal cell –derived factor-1–induced cell adhesion and chemotaxis in multiple myeloma

Abdel Kareem Azab, Feda Azab, Simona Blotta, Costas M. Pitsillides, Brian Thompson, Judith M. Runnels, Aldo M. Roccaro, Hai T. Ngo, Molly R. Melhem, Antonio Sacco, Xiaoying Jia, Kenneth C. Anderson, Charles P. Lin, Barrett J. Rollins and Irene M. Ghobrial

Updated information and services can be found at:

<http://www.bloodjournal.org/content/114/3/619.full.html>

Articles on similar topics can be found in the following Blood collections

[Lymphoid Neoplasia](#) (2898 articles)

Information about reproducing this article in parts or in its entirety may be found online at:

http://www.bloodjournal.org/site/misc/rights.xhtml#repub_requests

Information about ordering reprints may be found online at:

<http://www.bloodjournal.org/site/misc/rights.xhtml#reprints>

Information about subscriptions and ASH membership may be found online at:

<http://www.bloodjournal.org/site/subscriptions/index.xhtml>